

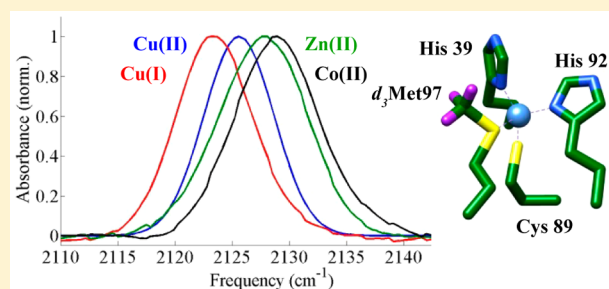
Methionine Ligand Interaction in a Blue Copper Protein Characterized by Site-Selective Infrared Spectroscopy

Amanda L. Le Sueur, Richard N. Schaugard, Mu-Hyun Baik,[†] and Megan C. Thielges*

Department of Chemistry, Indiana University, 800 East Kirkwood Avenue, Bloomington, Indiana 47405, United States

S Supporting Information

ABSTRACT: The reactivity of metal sites in proteins is tuned by protein-based ligands. For example, in blue copper proteins such as plastocyanin (Pc), the structure imparts a highly elongated bond between the Cu and a methionine (Met) axial ligand to modulate its redox properties. Despite extensive study, a complete understanding of the contribution of the protein to redox activity is challenged by experimentally accessing both redox states of metalloproteins. Using infrared (IR) spectroscopy in combination with site-selective labeling with carbon–deuterium (C–D) vibrational probes, we characterized the localized changes at the Cu ligand Met97 in the oxidized and reduced states, as well as the Zn(II) or Co(II)-substituted, the pH-induced low-coordinate, the apoprotein, and the unfolded states. The IR absorptions of (*d*₃-methyl)Met97 are highly sensitive to interaction of the sulfur-based orbitals with the metal center and are demonstrated to be useful reporters of its modulation in the different states. Unrestricted Kohn–Sham density functional theory calculations performed on a model of the Cu site of Pc confirm the observed dependence. IR spectroscopy was then applied to characterize the impact of binding to the physiological redox partner cytochrome (*cyt*) *f*. The spectral changes suggest a slightly stronger Cu–S(Met97) interaction in the complex with *cyt f* that has potential to modulate the electron transfer properties. Besides providing direct, molecular-level comparison of the oxidized and reduced states of Pc from the perspective of the axial Met ligand and evidence for perturbation of the Cu site properties by redox partner binding, this study demonstrates the localized spatial information afforded by IR spectroscopy of selectively incorporated C–D probes.



INTRODUCTION

Metal sites in proteins serve essential roles in biological function. To suit their particular role, metalloproteins can tailor their activity through control of protein-based metal ligands. For example, the Cu site in type I blue Cu proteins, named for their unusual spectral features, show heightened midpoint potentials compared to small molecule Cu systems attributed to the distinct coordination environment created by the protein.¹ One intensively studied blue Cu protein is plastocyanin (Pc), found in the thylakoid lumen of plants or the cytoplasm of cyanobacteria, where it shuttles electrons between cytochrome (*cyt*) *f* and photosystem I. In Pc, the Cu is ligated by four protein-based ligands: cysteine (Cys), methionine (Met), and two histidines (His) ligands (Figure 1). A hallmark of Cu centers in blue Cu proteins such as Pc is a short Cu–S(Cys) bond of ~2.1 Å that combined with an unusually long Cu–S(Met) bond of ~2.9 Å creates a distorted tetrahedral coordination geometry. This geometry is thought to result from a weak interaction between Cu and the Met axial ligand, which in turn induces Cu–S(Cys) orbital mixing and a shorter and stronger Cu–Cys bond, to result in the characteristic strong visible absorption spectrum² and possibly optimized midpoint potential, reorganization energy, and/or electron transfer (ET) pathway through the protein.^{3,4} In addition to the impact of a metalloprotein itself in dictating the metal

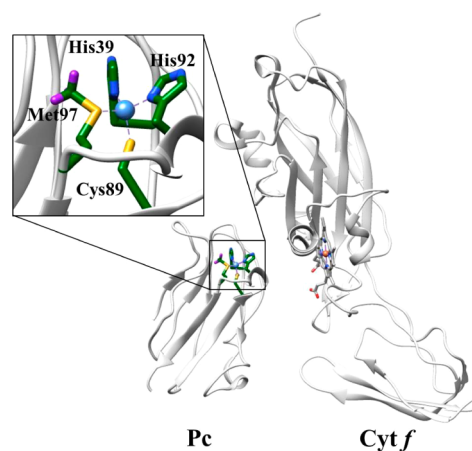


Figure 1. Structural model of the Pc–*cyt f* complex (PDB 1TU2).⁶ Inset: expanded view of the Cu site of Pc with introduced deuteriums at Met97 highlighted in purple.⁷

environment, the binding by redox partners can alter the ET properties.⁵ Thus, fully understanding the Pc function and the protein's role in modulating metal center reactivity requires a

Received: April 15, 2016

Published: May 10, 2016

complete assessment of Cu–S(Met) and other metal–ligand bonds and how they change in the biological redox reaction.

Pc and other blue copper proteins have been extensively studied and their electronic structures in the oxidized state illuminated via visible, electron paramagnetic resonance (EPR), and magnetic circular dichroism spectroscopy.⁴ However, the literature is nearly devoid of experimental studies of the reduced state because its filled d orbitals preclude characterization by most spectroscopic methods. The few examples include the application of X-ray absorption spectroscopy (XAS), but unfortunately, the contribution from the Cu–S(Met) bond in the free protein was undetectable or ambiguous.^{5,8} Photoelectron spectroscopy is applicable for characterization of reduced Cu sites, but is only experimentally feasible with small molecule biomimetic complexes.⁹ Crystal structures of oxidized and reduced proteins discern lengthening of Cu–ligand bonds in the reduced state for most Pc homologues, although the differences are very small (~ 0.1 Å).^{10,11} Thus, characterization of the reduced state has been challenging, and methods to address this limitation are desirable.

Toward generating a more complete understanding of the Cu site of Pc, we applied infrared (IR) spectroscopy in combination with selective labeling with carbon–deuterium (C–D) bonds to achieve localized characterization of Pc from the perspective of the Met axial ligand. Because IR spectroscopy probes vibrational rather than electronic transitions, it is applicable to both redox states. Additionally, the use of approximately local mode vibrations such as C–D bonds as IR probes enables characterization of one distinct location in Pc with high spatial precision, and the inherent fast time scale of IR spectroscopy ensures resolution of all heterogeneity in the environment of the C–D probe (via inhomogeneous line width broadening) as the interconversion of all protein conformational states is expected to be slow on the IR time scale. While the complexity and congestion of the vibrational spectra challenge the application of IR spectroscopy for the study of proteins, site-selective incorporation of groups such as C–D bonds that absorb in a “transparent” spectral region (~ 1900 – 2300 cm^{-1}) provides frequency-resolved vibrational bands that can be accurately analyzed to characterize local sites in proteins.¹² Moreover, incorporation of C–D bonds as IR probes in proteins is completely nonperturbative, which is an especially important consideration for the study of metal centers and their ligands as small perturbations can have large effects on their properties. Previously, the C–D vibrations of (*d*₃-methyl)methionine have been demonstrated as useful probes of local environmental changes in the proteins cytochrome *c* and dihydrofolate reductase.^{12–18} The absorption frequencies of C–D bonds are sensitive to electronic perturbation at adjacent heteroatoms,¹² suggesting that the CD₃ group should be a sensitive probe of the interactions between Met97 and the Cu center of Pc.

We site-specifically introduced (*d*₃-methyl)methionine at the axial ligand position 97 in *Nostoc* cyanobacterial Pc (*d*₃-Met) as a local IR reporter of the Cu site. Unique incorporation required removal of initiator Met1 and the only other methionine residue Met66. Met1 was removed via substitution of the two residues after the initiator methionine with alanine in combination with coexpression of methionine aminopeptidase,¹⁹ and Met66 was removed via mutagenesis to leucine. Expression of the modified Pc in minimal media containing (*d*₃-methyl)methionine enabled unique labeling at Met97. We then

utilized the C–D vibrations to probe the interaction of the Met97 ligand with the Cu center of Pc. Despite the long and presumably weak Cu–S(Met) bond, the IR spectra show that the ligand is highly sensitive to the nature of the metal center, help elucidate the underlying interactions, and furthermore suggest that they are sensitive to the binding of the protein's physiological redox partner, *cyt f*.

METHODS AND MATERIALS

Sample Preparation. The leader sequence (first 34 amino acids) of the *petE* gene encoding Pc in *Nostoc* PCC7119 was removed to achieve cytoplasmic expression according to literature procedures.²⁰ The truncated gene was subcloned as an *NdeI*–*XhoI* restriction fragment into vector pET28a. To ensure expression of Pc containing a unique methionine at position 97 (*d*₃-Met97 Pc), two alanine codons were introduced after the initiator methionine codon and Pc was coexpressed with methionine aminopeptidase (using plasmid pMetAP-GTG-21a¹⁹) to promote removal of the initiator methionine residue. In addition, the only other methionine of Pc, Met66, was substituted with leucine using site-directed mutagenesis. The integrities of the final plasmid construct and the expressed Pc were verified by DNA sequencing and mass spectrometry, respectively. The same amino acid numbering for the modified Pc [hereafter referred to as Pc] was used as derived from PDB entry 1TU2 for *Nostoc* Pc and excludes the initial methionine and the non-native precursor sequence “MAA-” for clarity when comparison is made to literature numbering. The expressions of Pc and *cyt f*²¹ were performed as described in the literature with minor modifications. Pc was expressed in minimal media containing supplemented M9 minimal salts and a 400 mg/L concentration of each amino acid excluding methionine. The media also contained either 400 mg/L methionine or 50 mg/L (*d*₃-methyl)methionine (Cambridge Isotopes) for expression of unlabeled or *d*₃-Met97 Pc, respectively. Preparation of Pc with Cu substituted by Zn(II) or Co(II) and in the unfolded, apoprotein, and low-pH states proceeded with established protocols, which are described in detail in the Supporting Information. FT IR data of all proteins and Pc–*cyt f* protein complexes with the exception of the unfolded and apoprotein states were taken in low ionic strength (1 mM) sodium phosphate buffer. For comparison, FT IR data were also taken of the oxidized and reduced Cu protein, as well as the Zn(II)- and Co(II)-substituted Pc, under buffer conditions identical to those used for the unfolded and apoprotein states, and can be found in the Supporting Information. All protein variants were characterized with circular dichroism and UV–vis spectroscopy (Figures S2–S4).

FT IR Measurements. FT IR spectroscopy was performed with an Agilent Cary 670 FT IR spectrometer using a liquid nitrogen cooled mercury–cadmium–telluride detector at 4 cm^{-1} resolution at 2000 cm^{-1} . IR absorption spectra of *d*₃-Met97 Pc were generated using transmission spectra of unlabeled and labeled Pc acquired under identical conditions. For both the reference and sample, 10000 scans were averaged after the chamber was purged with dry nitrogen for 30 min. Experiments were performed using a band-pass filter (Thorlabs FB4500-500) with a center frequency of 4500 nm and full width at half-maximum (fwhm) of 500 nm. The spectra were generated using a Blackman–Harris function for apodization, a zero filling factor of 8, and the Mertz phase correction algorithm. All experiments were performed in at least triplicate. A residual slowly varying baseline in the absorption spectra was removed by fitting a polynomial to a spectral region of ~ 200 cm^{-1} excluding the *d*₃-Met absorption bands (Matlab 7.8.0). The CD₃ symmetric stretch absorptions of the baseline-corrected spectra were then fit to a Gaussian or sum of Gaussian functions (Supporting Information).

Calculations. Unrestricted Kohn–Sham density functional theory (DFT) calculations were performed with the quantum chemical program package ORCA 3.0.3²² using the hybrid exchange–correlation functional B3LYP and PBE0. Ahlrich's def2-SVP basis set was utilized for geometry optimizations and vibrational mode calculations.²³ H–D isotope shifts for vibration calculations were obtained by changing the

mass of the hydrogens of interest to 2.0141 au and performing a normal-mode analysis using the existing Hessian.

For computational expediency a small model was obtained by truncating a crystal structure of *Nostoc* Pc (PDB 2GIM) to the immediate coordination environment of Cu. The two metal-bound His sites were replaced by imidazole ligands, Met was represented by ethyl methyl sulfide, and Cys was modeled by methanethiolate (Figure S8).

Free geometry optimization of the small model of the Cu site failed to produce a structure where ethyl methyl sulfide remained attached to the Cu center, indicating that the coordination geometry is enforced by the protein. To simulate this effect, all the bond angles of the metal-bound ligand atoms where Cu was the central atom were constrained to the values obtained in the crystal structure. Imaginary modes resulting from this procedure were very small, suggesting that this is a reasonable protocol from a computational perspective. Any imaginary modes present in the resulting structures were eliminated by manually displacing the structure along the offending mode(s).

A larger structure was also formed by truncating the same crystal structure in a way that preserved much of the H-bonding interactions with the ligands in the secondary coordination sphere (Figure S9). These structures did not require constraints to converge to minima and did not return imaginary modes.

RESULTS AND DISCUSSION

Nostoc d₃-Met97 Pc was generated by a combination of mutagenesis and methionine aminopeptidase coexpression in labeled media. The FT IR spectra of *d₃-Met97* Pc show bands at frequencies expected for the CD₃ symmetric and asymmetric stretches.¹⁴ For analysis, we focus on the symmetric stretches (Figure 2a) due to their increased intensity, which enables determination of the band frequencies and line widths with typically less than 0.1 and 0.3 cm⁻¹ standard deviations, respectively (Table 1). For both oxidation states, the absorptions are well fit by single Gaussian bands (Figure S5),

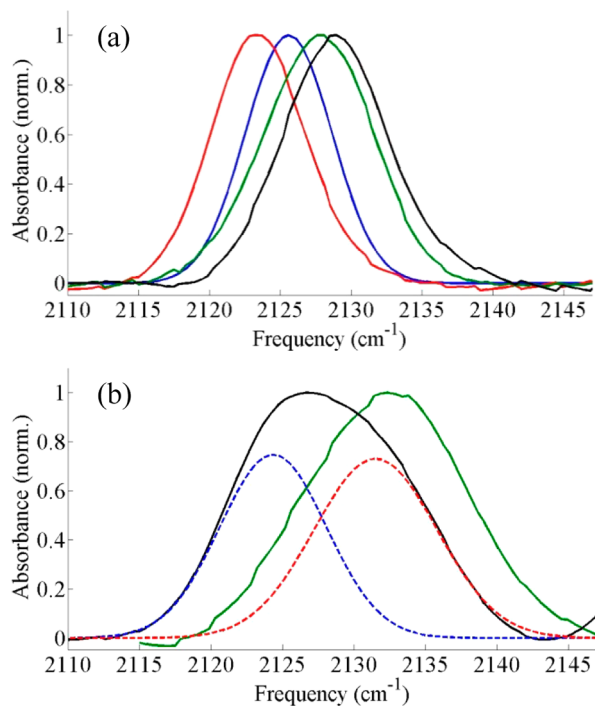


Figure 2. (a) FT IR spectra of *d₃-Met97* of Cu(I)Pc (red), Cu(II)Pc (blue), Zn(II)Pc (green), and Co(II)Pc (black). (b) FT IR spectra of *d₃-Met97* of ApoPc (black) and unfolded Pc (green). Gaussian components from fits to ApoPc are shown as blue and red dashed lines.

suggesting population of a single conformation in either state. Both absorptions appear at relatively low frequencies. The frequency for the reduced state is 2123.3 cm⁻¹, and upon oxidation shifts to higher frequency by 2.4 cm⁻¹ to 2125.7 cm⁻¹. The C–D absorption for reduced Pc is the most red-shifted observed of any reported *d₃-Met* absorption in a protein (2125.2–2133.2 cm⁻¹) or in solutions of varying dielectric constant, which range from 2127.3 cm⁻¹ for the BOC-protected amino acid in toluene to 2135.4 cm⁻¹ for the unprotected amino acid in water.^{12–18} The bands are also relatively narrow, with fwhm values of 7.6 and 7.7 cm⁻¹ for the oxidized and reduced states, respectively, similar to those found for *d₃-Met* in highly homogeneous environments within the packed interior of proteins.^{12–18}

To assess the contribution of the folded protein environment to the C–D spectra, we prepared Pc in both the unfolded state and the apoprotein (ApoPc). Upon unfolding by addition of 6 M guanidinium hydrochloride, the C–D absorption shifts (by 6 and 9 cm⁻¹ for oxidized and reduced states, respectively) to a higher frequency of 2132.3 cm⁻¹ and broadens in line width by 5 cm⁻¹ to 12.6 cm⁻¹ (Figure 2b, Table 1). Similarly large blue shifting and line width broadening, reflective of a transition to a more polar and heterogeneous environment, are observed for *d₃-Met80* of cytochrome *c* upon guanidinium-induced unfolding.^{17,24}

ApoPc was prepared as described in the literature by treatment of the holoprotein with KCN in solutions of high NaCl concentration.²⁵ The spectra of the *d₃-Met97* in these samples are best fit by a sum of two absorption bands. One band appears at relatively high frequency (2131.6 cm⁻¹) and is relatively broad (10.6 cm⁻¹), so we assign it to a population of unfolded protein. A second band is found at lower frequency (2124.4 cm⁻¹) and is relatively narrow (8.9 cm⁻¹), which we assign to the folded state of ApoPc. The relative integrated areas of the two bands depend on the apoprotein preparation (Supporting Information). The lower frequency band assigned to ApoPc contributes most greatly when the sample is prepared in 1 M NaCl, in which case the relative band areas indicate that the folded ApoPc makes up ~50% of the population. Circular dichroism spectroscopy of the ApoPc sample agrees with this composition (Supporting Information). The frequency for ApoPc is intermediate between those for the oxidized and reduced holoprotein, and all are substantially red-shifted compared to that of the unfolded state. Thus, the folded environment itself, and not ligation to the metal center, underlies the induced red shift. This in turn suggests that the binding site is very nonpolar. The larger line width found for ApoPc compared to the holoprotein however suggests that ligation significantly reduces the conformational freedom of the side chain.

Finding that the low frequencies for *d₃-Met97* in the holoprotein generally stem from the nonpolar environment within the folded protein, we next sought a better understanding of the blue shift of the *d₃-Met97* absorption upon Pc oxidation. The unusual structure of the Cu center in Pc has focused attention on the interaction with the Cys ligand, which is known to be strongly coupled to the oxidized metal center.^{2,4,26–28} The major contribution to the covalent bonding in the Cu(II)Pc is attributed to mixing of the Cu 3d_{x²-y²} orbitals with 3pπ orbitals of Cys, and to a lesser extent with the two His ligands, while the contribution of Met is thought to be only minor.^{4,26,27,29,30} Reduction fills the Cu 3d_{x²-y²} orbital that is engaged in an antibonding interaction with the Cys ligand, thus

Table 1. Parameters from Gaussian Fits to Experimental Spectra and Computational Analysis for the d_3 -Met97 Symmetric Stretch^a

species	experimental		crystal structure data, Pc/ pseudoazurin	computational (PBE0)
	ν (cm ⁻¹)	fwhm ^b (cm ⁻¹)		
Cu(I)Pc	2123.3 ± 0.1	7.7 ± 0.1	2.9 ¹¹ /2.8 ³⁵	2195.4
Cu(II)Pc	2125.7 ± 0.1	7.6 ± 0.1	2.8 ¹⁰ /2.7 ³⁵	2200.1
ZnPc	2127.7 ± 0.04	9.2 ± 0.4	NA/2.6 ³⁶	2204.4
CoPc	2128.8 ± 0.1	8.4 ± 0.6	NA/2.5 ³⁷	2201.8
ApoPc	2124.4 ± 0.4 (44%), 2131.6 ± 0.3 (56%)	8.9 ± 0.01, 10.6 ± 1.8		
unfolded Pc	2132.3 ± 0.1	12.6 ± 1.2		
Cu(I)Pc, pH 4	2123.2 ± 0.4 (66%), 2128.4 ± 1.5 (34%)	7.2 ± 1.0, 7.9 ± 0.3		
Cu(I)Pc-cyt <i>f</i> -bound	2123.6 ± 0.1	7.5 ± 0.2		
Cu(II)Pc-cyt <i>f</i> -bound	2126.1 ± 0.03	6.6 ± 0.2		

^aPercentages denote relative areas for Gaussian components. ^bFull width at maximum peak height.

decreasing the Cu–S bond order. Self-consistent field $X\alpha$ -scattered wave calculations on models of the oxidized and reduced states find the potential for interaction of Met sulfur-based orbitals with the $3d_{z^2}$ orbital of Cu in a pseudo- σ bond, but the orbital mixing is very minor in either state.^{26,29} Thus, the Cu–S(Met97) bond likely differs in Cu(II)Pc and Cu(I)Pc through primarily ionic interactions, which consequently should dominate the spectral changes of d_3 -Met97. However, the strength of the Cu–S(Met97) interaction in turn can be affected by the Cu–S(Cys89) bonding, as a compensatory relationship is observed between the two.

Because oxidation of Cu(I)Pc to Cu(II)Pc leads to changes in both metal charge and electronic configuration, unraveling the contributions to the differences in the C–D absorptions is difficult. To do so, we prepared and characterized Pc with the Cu site substituted by either Zn(II) or Co(II) (Zn(II)Pc and Co(II)Pc), as well as in the low-pH state of Cu(I)Pc. Both the Cu(I)Pc and Zn(II)Pc contain metal centers with d^{10} configurations, and differences in the bonding in these species should be primarily ionic in nature. Thus, comparison of these samples enables isolation of the spectral changes due to effectively doubling the metal charge in the absence of effects due to d orbital mixing. Additionally, at low pH the His92 ligand dissociates from the metal center of Cu(I)Pc, a change thought to serve as a regulatory response to conditions of potentially damaging light levels during photosynthesis,³¹ leaving a three-coordinate site with a contracted Cu–S(Met97) bond.¹¹ In this state the Cu(I) maintains the same charge and electronic configuration, but the decreased distance from Met97 should strengthen their ionic interaction. In contrast, the Co(II)Pc, Cu(II)Pc, and Zn(II)Pc have the same formal 2+ charge, although the effective nuclear charge, Z_{eff} , increases slightly across this series. These metal ions more dramatically differ in electronic structure. Unlike the d^9 configuration of Cu(II)Pc, Zn(II)Pc is a d^{10} system, whereas Co(II)Pc is a d^7 system. We attempted to prepare Ni(II)-substituted Pc, but were ultimately not successful, consistent with previous reports.³² Comparison of this series of analogous species helps to delineate the spectral effects associated with covalent interactions involving the protein-based ligands and the metal center.

To understand the differences in the C–D frequencies of the Pc variants, we first consider Cu(I)Pc and Zn(II)Pc, the d^{10} systems intended to isolate the influence of metal charge. The Zn(II)Pc shows a C–D absorption at a relatively high frequency of 2127.7 cm⁻¹. The additional positive charge at

the metal increases the C–D frequency by 4.4 cm⁻¹. To further assess the relationship between the C–D frequency and ionic interaction of Met97 with the Cu center, we characterized the low-pH state of Cu(I)Pc, which contains a three-coordinate metal center with a shorter Cu(I)–S(Met97) bond. The IR spectrum of this sample is best fit by a sum of two bands (Figure 3). A dominant band (66% relative area) appears at

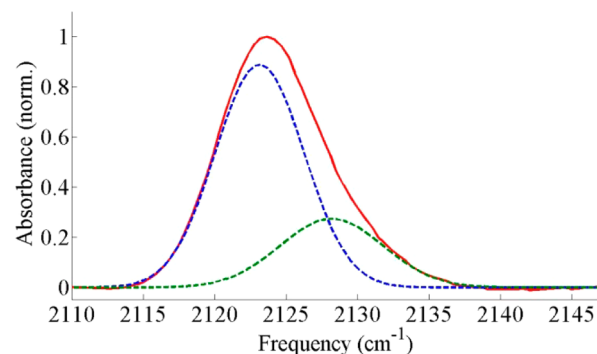


Figure 3. FT IR spectra of d_3 -Met97 of Cu(I)Pc at pH 4 (red). Gaussian components from fits are shown as blue and green dashed lines.

2123.2 cm⁻¹, within the error of the frequency observed for reduced Cu(I)Pc at pH 7. A second band (34% relative area) is shifted to higher frequency by 5.2 cm⁻¹. We assign this higher frequency band to the His92-dissociated state. The 34% population of the dissociated state indicated by the relative integrated band area differs from what a simple calculation based on the apparent pK_a of 5.09³³ of His92 would predict, namely, a population of the dissociated state of ~90%. This mismatch must be evaluated with caution, however, given how sensitive population differentials are to slight energy changes and considering some of the innate uncertainties in the measurements: the potential variation in the C–D cross sections is relatively large, accurate peak integration is challenging, and the steepness of the pH titration curve near a side chain's pK_a introduces significant errors. Interestingly, no differences in the IR spectrum were observed at pH 4 for Cu(II)Pc, which does not undergo the acid-induced transition (Supporting Information). Thus, formation of three-coordinate Cu(I) at low pH also blue shifts the CD₃ symmetric absorption (by 5.2 cm⁻¹). This is in agreement with the Cu(I)Pc/Zn(II)Pc data that indicate formation of a stronger ionic interaction

between the metal and Met97 engenders a blue shift of the C–D frequency, whether due to increased metal charge or a decreased interaction distance.

These results likewise imply that the more positively charged metal centers of Cu(II)Pc and Co(II)Pc compared to Cu(I)Pc should contribute to blue shifting of the C–D frequencies. Indeed, the spectrum of the Co(II)Pc shows a C–D absorption at a high frequency of 2128.8 cm⁻¹. However, the effect of the charge of the metal alone does not fully explain the differences. Consideration of the expected Z_{eff} of the metals predicts that the frequencies for Co(II)Pc, Cu(II)Pc, and Zn(II)Pc should slightly increase across the series but vary only marginally relative to their difference from Cu(I)Pc, which is contrary to experimental observation. Instead, the span in the C–D frequencies among these species (3 cm⁻¹) is substantial compared to the 4.4 cm⁻¹ difference between Zn(II)Pc and Cu(I)Pc. In addition, Co(II) is expected to have the smallest Z_{eff} of the metal series, but the C–D absorption for Co(II)Pc shows the highest frequency.

Since consideration of metal charge alone cannot fully explain the spectral differences among the Pc variants, we examined the potential contribution from bond covalency. Both Co(II) and Cu(II) have partially unoccupied 3d orbitals that may mix with protein side chains that act as ligands. Co(II)Pc contains a metal center with partially unoccupied $d_{x^2-y^2}$, d_{xy} , and d_z^2 orbitals. Unlike Cu(II)Pc, the interaction of Cys89 with the $d_{x^2-y^2}$ orbital of Co(II) is expected to be weak.^{32,34} Instead, the dominant covalent interaction of Cys89 with Co(II) involves a σ interaction with the d_{xy} orbital; however, the relative intensities of the corresponding visible absorptions indicate the σ interaction with Co(II) is weaker than the π interaction of Cu(II) with Cys89.³² The mixing of the occupied Cys89 orbital with an unoccupied Cu(II) orbital would decrease the magnitude of positive charge at the metal, and so is predicted to be associated with a decrease in the C–D frequency. This is contrary to our observation that the C–D frequency for Co(II)Pc is higher than that for Zn(II)Pc. Importantly, in contrast to the Cu(I/II) and Zn(II) proteins, in Co(II)Pc a covalent interaction between the Co(II) and Met97 itself potentially contributes to the spectrum. Distinctly, in Co(II)Pc, a partially occupied d_z^2 orbital is available and aligned to interact with the sulfur-based orbitals of Met97. Because the interaction of the orbitals of Met97 with the unoccupied metal orbitals is likely to have a stabilizing effect similar to that of the ionic interaction with the metal charge, it is expected to result in similar blue shifting of the C–D frequency. Therefore, we attribute the high frequency of the C–D band for the Co(II)Pc to the combined effects of its sensitivity to the positive metal charge and increased orbital mixing of Met97 uniquely with Co(II).

With a better understanding of the contributions to the frequency changes of the C–D absorption for the Pc variants, we reconsider the spectral differences associated with oxidation. As already discussed, metal–S(Met97) covalent interactions are not predicted to substantially contribute to the differences in metal binding with Cu(I)Pc, Cu(II)Pc, or Zn(II)Pc, so in these proteins the C–D absorption should primarily report on changes in the strength of the ionic interaction of Met97 with the positively charged metal center. In agreement with this, the IR data do not suggest mixing of the singly occupied $d_{x^2-y^2}$ orbital of Cu(II) with those of Met97, as the C–D frequency is lower for Cu(II)Pc than Zn(II)Pc, rather than higher as found for Co(II)Pc, which has the partially occupied d_z^2 orbital

oriented for interaction with Met97. The dominant covalent interaction in Cu(II)Pc involves mixing of an occupied Cys89 orbital with a partially unoccupied orbital of Cu(II), which results in significant charge transfer from the Cys89 ligand to the metal. Consequently, the Cu–S(Cys89) interaction is expected to reduce the effective positive metal charge felt by d_z^2 -Met97 to a value intermediate between those for Cu(I)Pc and Zn(II)Pc. Given the positive correlation between the magnitude of positive metal charge and frequency indicated by the data for Cu(I)Pc and Zn(II)Pc, the intermediate frequency observed for the Cu(II) protein is in line with the intermediate effective metal charge felt by Met97 when the effect of Cu(II)–Cys89 covalent bonding is considered. The magnitude of the frequency difference associated with this effect is notably substantial. In comparison to the 4.4 cm⁻¹ lower C–D frequency associated with an approximate decrease of one unit of positive metal charge from Zn(II)Pc to Cu(I)Pc, a 2 cm⁻¹ lower C–D frequency is found for Cu(II)Pc than for Zn(II)Pc. Thus, the magnitude of the frequency shift attributed to Cu(II)–S(Cys89) covalent mixing is nearly half as large as results from a decrease in one unit of charge at the metal. Interestingly, this is consistent with combined theoretical and experimental data which suggest that the highest occupied molecular orbital (HOMO) of Cu(II)Pc possesses ~40% Cys 3p π character.³⁴ Thus, the IR data indicate a very strong Cu(II)–Cys89 covalent interaction.

In addition to the frequency differences among the metal series of Pc, the absorption line widths for Zn(II)Pc and Co(II)Pc are broader by 2 cm⁻¹ than found for the native Cu proteins. Assuming that the line width changes are dominated by inhomogeneous broadening, as is typically the case for absorptions in proteins,^{24,38} the broader line widths suggest greater heterogeneity in the metal-substituted Pc. This could be due to smaller force constants intrinsic to the metal–ligand bonds of Co(II) and Zn(II), as found in previous calculations of model complexes with these metals.³⁴

To confirm that the observed spectral changes reflect sensitivity to the positively charged metal, DFT were performed on a model of the metal site in Pc using the PBE0 and B3LYP functionals. A minimal model consisted of a metal ion carrying methyl sulfide, methanethiolate, and two imidazoles, as mimics of the Met, Cys, and His ligands, respectively. The bond angles were constrained to those observed in the crystal structures of Pc, and the Zn(II)Pc and Co(II)Pc models used the same starting geometry as the native Cu protein. Optimized geometries for the oxidized, reduced, Zn(II)Pc, and Co(II)Pc states are shown in Figure S8, and results from harmonic frequency calculations for the CD₃ group are reported in Tables 1 and S2. To assess secondary ligand sphere effects, larger models of the metal sites in all variants of Pc were generated by truncation of the crystal structures to include only the primary coordination environment and several hydrogen-bonding interactions found within the surrounding protein that were deemed likely to enforce the primary coordination environment (Figure S9). Whereas geometry optimization of the minimal models of the metal center in the absence of structural constraints did not converge to structures in which all the ligands remained attached, the larger models converged to structures that yielded C–D frequencies that replicated the trend found for the constrained minimal models (Table S2), suggesting that the secondary ligand sphere is necessary to maintain the structural integrity of the metal sites, but does not

otherwise contribute significantly to the observed differences in the C–D absorptions.

Compared to Cu(I)Pc, the calculated frequencies for all the other states (Cu(II)Pc, Zn(II)Pc, Co(II)Pc, and Cu(I) in the three-coordinate complex) are shifted to higher frequency, and thus generally reproduce the experimentally observed trend. In agreement with the empirical interpretation, the calculations suggest that the variation in C–D frequencies reflects their sensitivity to the positive charge of the metal. At the B3LYP-def2-SVP level of theory, the HOMO of ethyl methyl sulfide is almost entirely sulfur p in character, but also has contributions from the C–D σ and σ^* orbitals. Interaction of the Met97 with a more positively charged metal lowers the sulfur p orbital energy, allowing a better interaction with the C–D σ orbital compared to the σ^* orbital, which in turn increases the contribution of the C–D σ orbitals to the HOMO and leads to a higher C–D frequency (Figure S11). Consistent with this idea, modeling the interaction of the ethyl methyl sulfide with a point charge of varying magnitude recapitulates the trend in C–D frequencies (Table S3). As there were no basis functions centered on the point charge for these latter calculations, the calculated frequency trend exclusively reflects the influence of an ionic interaction.

Although the calculations generally capture the influence of the positive charge of the metal on the C–D frequency, they underestimate the frequency for Co(II)Pc. As this is the only complex in which the orbitals of Met97 have the potential to significantly mix with orbitals of the metal, it is possible that the calculations do not sufficiently capture the covalency of the Co(II)–Met97 interaction, which is likely to be highly sensitive to the metal site geometry used in the calculations. The experimentally determined frequencies do show an inverse correlation with the lengths of the metal–S(Met) bonds from crystal structures of Pc, which are available for all the species but the Zn(II)Pc and Co(II)Pc, or from structures of pseudoazurin, which contains the same ligand set as Pc,³⁹ which further supports that the IR spectra of d_3 -Met97 report on sensitivity to its interaction with the metal center. The spectral, computational, and structural data for the different species of Pc thus are compatible with the presence of a weak ionic interaction of Met97 with Cu(I), a stronger but still relatively weak ionic interaction with Cu(II) due to the strong covalent bonding of Cu–S(Cys89), a relatively strong ionic interaction with Zn(II), and a strong partially covalent interaction with Co(II).

Finally, to further test whether d_3 -Met97 is sensitive to changes that might contribute to biological function, we characterized the effects of binding the physiological redox partner, cyt *f* (Figure 4, Table 1). Whereas under physiological conditions reduced cyt *f* transfers an electron to oxidized Pc, we looked at the binding-induced changes with both proteins in the oxidized or reduced state to eliminate complications due to the redox equilibrium. For the oxidized and reduced states we observe small, but reproducible and significant, 0.4 and 0.3 cm^{-1} ($\pm <0.1 \text{ cm}^{-1}$) shifts in the d_3 -Met97 absorptions to higher frequency upon Pc–cyt *f* binding. This indicates that the effects of cyt *f* binding are transduced to Met97 at the metal site. The spectral changes are not likely dominated by the effect of surface water displacement by cyt *f* binding, which would cause the C–D probe to experience a more nonpolar environment and result in a red shift, contrary to observation. Alternately, our study of the metal series of Pc suggests that the blue shift upon cyt *f* binding reflects a stronger interaction

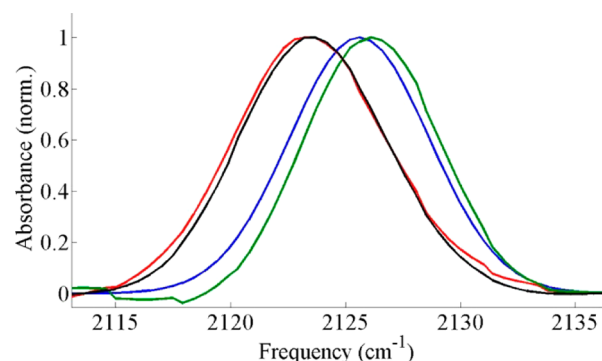


Figure 4. FT IR spectra of d_3 -Met97 of unbound Cu(I)Pc (red), unbound Cu(II)Pc (blue), cyt *f*-bound Cu(I)Pc (black), and cyt *f*-bound Cu(II)Pc (green).

between the Cu and Met97. A crude but illustrative comparison of the magnitude of the frequency change associated with cyt *f* binding finds it is $\sim 10\%$ that due to a change of one unit of metal charge. Consistent with this interpretation, XAS studies of oxidized and reduced Pc find spectral contributions from Cu–S(Met) in the complex with cyt *f* but not the free protein, which suggests formation of a shorter Cu–S(Met) bond in the complex.⁷

In addition, the C–D absorptions show a significant decrease (by 1 cm^{-1}) in line width upon binding cyt *f* in the oxidized state. This suggests that binding of Pc to cyt *f* leads to a more homogeneous environment at Met97, consistent with greater conformational restriction in the protein–protein complex. The absorption narrowing is found only for the oxidized protein complex, so the IR data report lower conformational heterogeneity in that state. XAS of the Pc–cyt *f* complex similarly finds different conformational restrictions for the oxidized and reduced states, but, in contrast to our study, reports greater restriction in the reduced state.^{5,8} Nevertheless, the IR data provide evidence that complexation with cyt *f* likely impacts the ET properties of Pc. Indeed, there are other examples of complexation with electron transfer partners influencing ET reactions.^{40,41}

Previous studies of a range of blue Cu proteins and their axial ligand mutants have identified an inverse correlation between the strength of an axial ligand interaction and the midpoint potential of the metal center.^{1,3} On the basis of this observation, an increase in the Cu(II)–Met97 interaction upon binding with cyt *f* suggested by the spectral data would predict a reduction in the midpoint potential. Interestingly, this aligns with previous measurement of a 30 mV decrease in the reduction potential for Pc in complex with cyt *f*.⁴² Additionally, the ET rates through possible pathways in proteins strongly depend on the coupling between the ligands connecting the pathway and the metal. One of two competing ET pathways specifically evoked in Pc is mediated through the Cu–S(Cys89) covalent bond.³ Given the compensatory relationship between the Met97 and Cys89 bonding with Cu(II), the stronger Cu–S(Met97) interaction potentially reflects a corresponding weaker Cu(II)–S(Cys89) bond, which could have a great impact on the contribution of the ET pathway mediated through it.

CONCLUSIONS

The data clearly reveal that the absorptions of the C–D bonds site-selectively incorporated at the Met axial ligand of Pc are sensitive to the nature of the Cu center. This sensitivity likely

results from variation in the interaction between sulfur-centered orbitals of Met97 and the positively charged metal center, which itself is influenced by interaction with the other ligands, presumably most significantly Cys89. The approach enables direct, nonperturbative, molecular-level comparison of the oxidized state to the reduced state of Pc, as well as to several other variants, with the same experimental method. Our spectral data support the presence of the strong covalent interaction between Cu(II) and Cys89, and that Met97 acts to stabilize the metal center via ionic interactions. The spectral changes observed upon binding cyt *f* suggest increased Cu–Met97 interaction in the complex, which illustrates a mechanism for the modulation of the ET properties from complexation with a redox partner. Further characterization of Pc, including the site-selective deuteration of other ligands, promises to more fully elucidate the nature of the Cu site and how it is modulated for function. Similarly, the IR characterization of ligands in other blue Cu proteins with varied metal sites and other proteins with presumably weak metal–ligand bonds should help illuminate how they contribute to tuning the reactivity for metalloproteins' specific function in biology.

■ ASSOCIATED CONTENT

📄 Supporting Information

The Supporting Information is available free of charge on the ACS Publications website at DOI: 10.1021/jacs.6b03916.

Experimental details of protein expression, spectroscopic measurement and fitting parameters, and computational details (PDF)

■ AUTHOR INFORMATION

Corresponding Author

*thielges@indiana.edu

Present Address

†M.-H.B.: Department of Chemistry, Korea Advanced Institute of Science and Technology, 291 Daehak-ro, Yuseong-gu, Daejeon 305-701, Republic of Korea.

Notes

The authors declare no competing financial interest.

■ ACKNOWLEDGMENTS

We thank Marcellus Ubbink (Leiden University) for providing expression plasmids for Pc and cyt *f*. A.L.L. and M.C.T. thank Indiana University and the Department of Energy (Grant DE-FOA-0000751) for funding.

■ REFERENCES

- (1) Gray, H. B.; Malmstrom, B. G.; Williams, R. J. P. *JBIC, J. Biol. Inorg. Chem.* **2000**, *5*, 551.
- (2) Solomon, E. I.; Hare, J. W.; Gray, H. B. *Proc. Natl. Acad. Sci. U. S. A.* **1976**, *73*, 1389.
- (3) Randall, D. W.; Gamelin, D. R.; LaCroix, L. B.; Solomon, E. I. *J. Biol. Inorg. Chem.* **2000**, *5*, 16.
- (4) Solomon, E. I.; Szilagyi, R. K.; DeBeer George, S.; Basumallick, L. *Chem. Rev.* **2004**, *104*, 419.
- (5) Diaz-Moreno, I.; Diaz-Quintana, A.; Diaz-Moreno, S.; Subias, G.; De la Rosa, M. A. *FEBS Lett.* **2006**, *580*, 6187.
- (6) Diaz-Moreno, I.; Diaz-Quintana, A.; De la Rosa, M. A.; Ubbink, M. *J. Biol. Chem.* **2005**, *280*, 18908.
- (7) Pettersen, E. F.; Goddard, T. D.; Huang, C. C.; Couch, G. S.; Greenblatt, D. M.; Meng, E. C.; Ferrin, T. E. *J. Comput. Chem.* **2004**, *25*, 1605.

- (8) Cruz-Gallardo, I.; Diaz-Moreno, I.; Diaz-Quintana, A.; De la Rosa, M. A. *FEBS Lett.* **2012**, *586*, 646.
- (9) Guckert, J. A.; Lowery, M. D.; Solomon, E. I. *J. Am. Chem. Soc.* **1995**, *117*, 2817.
- (10) Guss, J. M.; Bartunik, H. D.; Freeman, H. C. *Acta Crystallogr., Sect. B: Struct. Sci.* **1992**, *48*, 790.
- (11) Guss, J. M.; Harrowell, P. R.; Murata, M.; Norris, V. A.; Freeman, H. C. *J. Mol. Biol.* **1986**, *192*, 361.
- (12) Chin, J. K.; Jimenez, R.; Romesberg, F. E. *J. Am. Chem. Soc.* **2001**, *123*, 2426.
- (13) Cremeens, M. E.; Fujisaki, H.; Zhang, Y.; Zimmermann, J.; Sagle, L. B.; Matsuda, S.; Dawson, P. E.; Straub, J. E.; Romesberg, F. E. *J. Am. Chem. Soc.* **2006**, *128*, 6028.
- (14) Thielges, M. C.; Case, D. A.; Romesberg, F. E. *J. Am. Chem. Soc.* **2008**, *130*, 6597.
- (15) Sagle, L. B.; Zimmermann, J.; Dawson, P. E.; Romesberg, F. E. *J. Am. Chem. Soc.* **2004**, *126*, 3384.
- (16) Zimmermann, J.; Thielges, M. C.; Yu, W.; Dawson, P. E.; Romesberg, F. E. *J. Phys. Chem. Lett.* **2011**, *2*, 412.
- (17) Sagle, L. B.; Zimmermann, J.; Matsuda, S.; Dawson, P. E.; Romesberg, F. E. *J. Am. Chem. Soc.* **2006**, *128*, 7909.
- (18) Chin, J. K.; Jimenez, R.; Romesberg, F. E. *J. Am. Chem. Soc.* **2002**, *124*, 1846.
- (19) Liao, Y.-D.; Jeng, J.-C.; Wang, C.-F.; Wang, S.-C.; Chang, S.-T. *Protein Sci.* **2004**, *13*, 1802.
- (20) Scanu, S.; Forster, J.; Finiguerra, M. G.; Shabestari, M. H.; Huber, M.; Ubbink, M. *ChemBioChem* **2012**, *13*, 1312.
- (21) Albarran, C.; Navarro, J. A.; Molina-Heredia, F. P.; Murdoch, P. d. S.; De la Rosa, M. A.; Hervas, M. *Biochemistry* **2005**, *44*, 11601.
- (22) Neese, F. *WIREs Comput. Mol. Sci.* **2012**, *2*, 73.
- (23) Schäfer, A.; Horn, H.; Ahlrichs, R. *J. Chem. Phys.* **1992**, *97*, 2571.
- (24) Thielges, M. C.; Zimmermann, J.; Dawson, P. E.; Romesberg, F. E. *J. Mol. Biol.* **2009**, *388*, 159.
- (25) Koide, S.; Dyson, H. J.; Wright, P. E. *Biochemistry* **1993**, *32*, 12299.
- (26) Gewirth, A. A.; Solomon, E. I. *J. Am. Chem. Soc.* **1988**, *110*, 3811.
- (27) Penfield, K. W.; Gay, R. R.; Himmelwright, R. S.; Eickman, N. C.; Norris, V. A.; Freeman, H. C.; Solomon, E. I. *J. Am. Chem. Soc.* **1981**, *103*, 4382.
- (28) Solomon, E. I.; Clendening, P. J.; Gray, H. B.; Grunthaner, F. J. *J. Am. Chem. Soc.* **1975**, *97*, 3878.
- (29) Penfield, K. W.; Gewirth, A. A.; Solomon, E. I. *J. Am. Chem. Soc.* **1985**, *107*, 4519.
- (30) Scott, R. A.; Hahn, J. E.; Doniach, S.; Freeman, H. C.; Hodgson, K. O. *J. Am. Chem. Soc.* **1982**, *104*, 5364.
- (31) Rochaix, J.-D. *Biochim. Biophys. Acta, Bioenerg.* **2011**, *1807*, 375.
- (32) McMillin, D. R.; Rosenberg, R. C.; Gray, H. B. *Proc. Natl. Acad. Sci. U. S. A.* **1974**, *71*, 4760.
- (33) Hass, M. A. S.; Thuesen, M. H.; Christensen, H. E. M.; Led, J. J. *J. Am. Chem. Soc.* **2004**, *126*, 753.
- (34) Gorelsky, S. I.; Basumallick, L.; Vura-Weis, J.; Sarangi, R.; Hodgson, K. O.; Hedman, B.; Fujisawa, K.; Solomon, E. I. *Inorg. Chem.* **2005**, *44*, 4947.
- (35) Libeu, C. A. P.; Kukimoto, M.; Nishiyama, M.; Horinouchi, S.; Adman, E. *Biochemistry* **1997**, *36*, 13160.
- (36) Gessmann, R.; Papadovasilaki, M.; Drougkas, E.; Petratos, K. *Acta Crystallogr., Sect. F: Struct. Biol. Commun.* **2015**, *71*, 19.
- (37) Gessmann, R.; Kyvelidou, C.; Papadovasilaki, M.; Petratos, K. *Biopolymers* **2011**, *95*, 202.
- (38) Chung, J. K.; Thielges, M. C.; Lynch, S. R.; Fayer, M. D. *J. Phys. Chem. B* **2012**, *116*, 11024.
- (39) Dennison, C. *Dalton Trans* **2005**, *21*, 3436.
- (40) Drepper, F.; Hippler, M.; Nitschke, W.; Haehnel, W. *Biochemistry* **1996**, *35*, 1282.
- (41) Roncel, M.; Boussac, A.; Zurita, J. L.; Bottin, H.; Sugiura, M.; Kirilovsky, D.; Ortega, J. M. *JBIC, J. Biol. Inorg. Chem.* **2003**, *8*, 206.
- (42) Malkin, R.; Knaff, D. B.; Bearden, A. J. *Biochim. Biophys. Acta, Bioenerg.* **1973**, *305*, 675.